JOURNAL OF MATERIALS SCIENCE 33 (1998) 1769–1775

Internal friction of foamed aluminium in the range of acoustic frequencies

C. S LIU, Z. G. ZHU, F. S. HAN
Laboratory of Internal Friction and Defects in Solids, Institute of Solid State Physics, Chinese Academy of Sciences, Hefei 230031, People's Republic of China
E-mail: zgzhu@issp.hfcas.ac.cn

J. BANHART
Fraunhofer Institute for Applied Materials Research, Lesumer Heerstrasse 36, 28717 Bremen, Germany

The internal friction of aluminium foams with various porosities was measured in the range of acoustic frequencies over a wide strain-amplitude range by the bending-vibration method. The measured internal friction shows that aluminium foams have a damping capacity which is enhanced in comparison with bulk aluminium, increases with increasing porosity, decreases with increasing frequency and increases with increasing strain amplitude. In order to explain the behaviour of the internal friction, a mechanism of internal dissipation energy was presented, and an approximate expression for internal friction is derived which is based on the equations of plane waves in elastic material with voids. This expression can account for the dependence of the internal friction on porosity, pore size and frequency. To gain further insight into the dependence of the internal friction on amplitude, the non-linear characteristics of oscillations were observed, and it was found that the resonance curves are asymmetric and the resonant frequencies are proportional to the square of amplitude with a negative slope. On the basis of the equations of the motion and the experimental results, the non-linearity of oscillations was ascribed to a non-linear damping term and an approximate expression for the damping coefficient with respect to amplitude was obtained.

1. Introduction

Foamed metals are earning growing attention as engineering materials. These exceptionally light-weight materials possess a unique combination of properties, such as impact energy absorption capacity, air and water permeability and favourable sound absorption properties, and are expected to help engineers to improve the performance of many products. There are many methods available to produce foamed metals, including casting, power metallurgy, metallic deposition and sputter deposition [1]. Aluminium (Al) has been chosen as the foaming material because of its lightness, low melting point and other favourable properties.

Foamed Al has a good machinability and formability and shows excellent antiweather properties. It is now expected to be used not only as a building material but also as a new functional material for noise reduction or as energy-absorbing material in cars.

The mechanical properties of metallic foams are of practical and scientific importance. Although there have been a great deal of studies on these properties using various techniques, studies using the internal friction have hardly appeared in the literature (see, for example, [2, 3]). Foamed Al is considered as a potential material for noise protection components in many applications of lightweight structures. Hence it is important to measure the internal friction (IF) of foamed Al in the acoustic frequency range. In the present paper, we measure the dependence of IF of foamed Al on its porosity, the applied frequency and the amplitude of vibration. We also discuss the reasons for the IF behaviour observed and for the non-linearity of oscillations.

2. Experimental procedure

2.1. Specimens

The specimens denoted FAl* were prepared by a powder-metallurgical foaming technique at Fraunhofer institute [4]. Metal or alloy powder was mixed with a small amount of foaming agent. The mixture was then compacted, resulting in a semifinished product in which the foaming agent was distributed homogeneously. Metal foam parts were then obtained by heating the semifinished material to its melting point. The specimens denoted FAl were fabricated by the slurry foaming technique [5, 6] at the Laboratory of Internal Friction. Foamed Al was fabricated by adding fine Al powder to a mixture consisting mainly of aluminium hydroxide and orthophosphoric acid. To increase the mechanical strength of foamed Al, the following measures were taken.

(i) Since oxidation film is harmful to sintering, Al powder was tumbled in a ball mill.

(ii) The mixture of Al powder and foaming agent was pressed before foaming.

(iii) Al foams were given a pre-sintering at 300 °C for 30 min and sintering treatment in vacuum at temperatures slightly below the melting point of Al for 120 min.

Because of (ii), we could not produce higher-porosity foams. The size of all specimens was cut to 73 mm × 3–8 mm × 3–5 mm.

2.2. Measurements

The IF was measured by means of a flexural vibration method. The specimen was freely suspended at the first resonance node with a fine wire. One end of the specimen was vibrated at a constant amplitude by a magnetic drive. The amplitude of free attenuation was measured with a magnetic detector after cutting off the driving power [7]. The frequencies of vibration are given by

$$f = \frac{2\alpha^2 R}{\pi l^2}\left(\frac{E}{\rho}\right)^{1/2} \quad (1)$$

where f is the vibration frequency, $\alpha = 0.752\,81\pi$ and R is the radius of gyration of a cross-section about the neutral axis of bending. The length, Young's modulus and specimen density are denoted by l, E and ρ, respectively. The IF was calculated as

$$Q^{-1} = \frac{K}{N} \quad (2)$$

where N is the number of free specimen vibrations corresponding to a definite lowering of their amplitude and K is an apparatus constant. The accuracy of the vibrational decay can be performed with a very high accuracy (1%). IF measurements were performed under vacuum at about 10^{-3} torr. The testing temperature was room temperature. The porosity of each specimen was calculated from measurements of its mass and volume. The pore size was calculated as the mean value of 20 individual pore diameter measurements on each specimen. According to Equation 1, the resonant frequency may be changed by changing the radius of gyration R, i.e., by changing its thickness.

3. Results and discussion

3.1. Internal friction of foamed Al, Zn–Al damping alloy and bulk Al

The experimental results for IF of three kinds of specimen at identical strain amplitudes are shown in Table I. Since the IF usually depends on frequency, the testing frequencies for different samples were chosen to be around 1000 Hz.

From Table I, conclusions may be drawn as follows: IF of foamed Al is about five times that of the Zn–Al damping alloy, and it is very much larger than that of bulk Al. The conclusions imply that attenuation in foamed Al is not caused by the usual machanism but by the pores.

It is widely accepted that any kind of porosity enhances damping owing to stress concentration and mode conversion around pores. This mechanism applies to microporosity as well as to the large pores found in metal foams [2, 8]. Especially in thin membranes, an external force, even when small, can lead to high multiaxial stresses. In other words, the elastic modulus of the pores differs from that of the matrix, which is called inhomogeneity inclusion [9]. When a force is imposed on the foamed Al, an inhomogeneous stress field, resulting from the inhomogeneity, is built up. Then, specific IF may arise from the inhomogeneous stress field to relax the stress concentration as soon as some irreversible process is actived. That is, the inhomogeneous stress field causes pore to dilate (or contract) and distort and, correspondingly, gives rise to the dilatation and distortion energy. The dilatation and distortion energy components transform to heat by dislocations and molecular collisions during cyclic movement. In addition, the movements of dislocations tend to end at pore surface where there is high surface energy converted from dislocation mobility. Therefore pores may be high-energy dissipation resources. The damping capacity of foamed Al is therefore higher than that of bulk Al.

TABLE I IF, Q^{-1}, for three kinds of specimen

Specimen	Frequency (Hz)	Porosity (%)	Pore size (mm)	$Q^{-1} \times 10^3$
FAI	992	65	0.8	9.1
FAI*	1005	82	1.5	7.3
Zn–Al	1001	0	0	1.7
Al	998	0	0	0.4

3.2. Relationship between internal friction and porosity

The experimental results on the relation between IF and porosity are shown in Table II. The testing frequencies of different samples were about 1000 Hz. The strain amplitudes of samples with different porosity are identical.

From Table II, we can see that the IF of foamed Al increases with increasing porosity. It also shows that pores may be high-energy dissipation resources for foamed Al. The higher the porosity, the larger is the stress concentration resulting from the inhomogeneity and the greater are the dilatation and distortion of pores due to the stress disturbance. From the consideration of Section 3.1, it is reasonable that the IF of foamed Al increases with increasing porosity.

3.3. Relationship between internal friction and frequency

For specimens FAl* and FAl, the values of IF are plotted against frequency in Fig. 1. The strain amplitudes are identical at different testing frequencies. The results shown in this figure suggest that the value of IF decreases with increasing frequency.

Foamed Al is composed of the metallic matrix and the pores. It is the elastic modulus difference between the matrix and the pores that results in a marked

TABLE II The relation between porosity and IF for FAI

Porosity	Pore size (mm)	Frequency (Hz)	$Q^{-1} \times 10^3$
0.52	0.8	1047	6.4
0.58	0.8	996	7.1
0.65	0.8	983	8.4
0.69	0.8	1089	8.8
0.76	0.8	1012	9.4

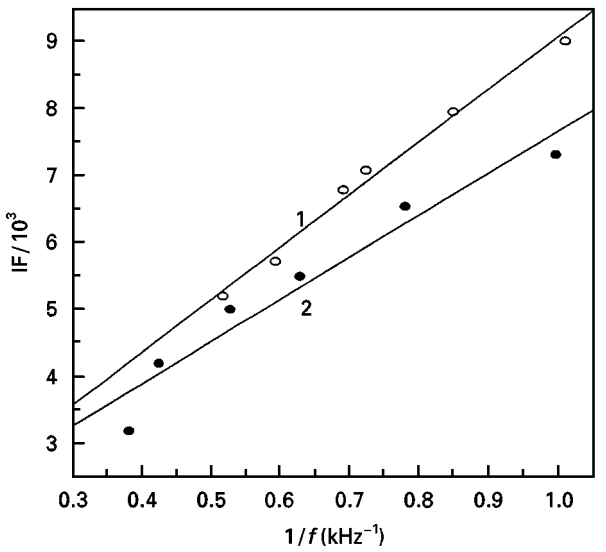

Figure 1 IF of FAI* (●) and FAI (○) for different frequencies. Line 1, $Y = 1.19 + 7.91X$; line 2, $Y = 1.35 + 6.35X$.

inhomogeneous stress field. When a bar is bent, stretching occurs at some points and compression at others, and the inhomogeneous stress field causes the dilatation and distortion of pores, which in turn cause the change in the local distribution of the matrix. The bulk density of foamed Al can be written as the product of two fields: the density field of the matrix Al and volume fraction field. The change in local volume fraction of the matrix from a reference value of the local volume fraction shows the dilatation and distortion of pores. The reference configuration is free of stress and strain. The greater the dilatation and distortion of pores, the larger is the change in local volume fraction.

The linear theory of elastic materials with pores deals with small changes from a reference configuration of a porous body [10–12]. In this configuration, the bulk density, ρ, matrix density, γ, and matrix volume fraction, v, are related by

$$\rho_r = \gamma_r v_r \tag{3}$$

$$v_r = \int v_r(\boldsymbol{x})\, dv \tag{4}$$

and the body is taken to be strain free. Here $\boldsymbol{x}$ is the spatial position vector in Cartesian coordinates, $v_r(\boldsymbol{x})$ is the local matrix volume fraction of a reference configuration, v is the volume and dv is the increment of v considered as tending to zero. The theory employs the same balance equations as proposed by Goodman and Cowin [10] and includes a rate effect in the volumetric response that may be due to inelastic surface effects in the vicinity of void boundaries. The independent kinematical variables in the linear theory are the displacement field, $u(\boldsymbol{x}, t)$, from the reference configuration and the change, $\phi(\boldsymbol{x}, t)$, in local volume fraction from the reference volume fraction

$$\phi(\boldsymbol{x}, t) = v(\boldsymbol{x}, t) - v_r(\boldsymbol{x}) \tag{5}$$

$$\int \psi(\boldsymbol{x}, t)\, dv = \int v_r(\boldsymbol{x})\, dv \tag{6}$$

where t is time. The parameter $\phi(\boldsymbol{x}, t)$ represents the dilatation and distortion of pores. The infinitesimal strain tensor, $\varepsilon(\boldsymbol{x}, t)$, is determined from the displacement field, u_i, according to

$$\varepsilon_{ij} = \tfrac{1}{2}(u_{i,j} + u_{j,i}) \tag{7}$$

where the comma followed by a lower-case Latin letter indicates a partial derivative with respect to the indicated coordinate.

The equations of motion for the medium considered are the balance of linear momentum

$$\rho \ddot{u}_j = T_{ij,j} + \rho b_i \tag{8}$$

and the balance of equilibrated force

$$\rho\kappa\ddot{\phi} = h_{i,i} + g + \rho l \tag{9}$$

Here T_{ij} is the symmetric stress tensor, b_i is the body force vector, h_i is the equilibrated stress vector, κ is the equilibrated inertia, g is the intrinsic equilibrated body force and ρl is the extrinsic equilibrated body force. These terms have been discussed in detail in [11, 13].

The constitutive equations for the linear isotropic theory of elastic porous materials relate the stress tensor, T_{ij}, the equilibrated stress vector, h_i, and intrinsic equilibrated body force, g, to the strain, ε_{ij}, the change, ϕ, in volume fraction, the time rate, $\dot{\phi}$, of change in the volume fraction and the gradient, $\phi_{,i}$, of the change in volume friction; thus

$$T_{ij} = \lambda\delta_{ij}\varepsilon_{kk} + 2\mu\varepsilon_{ij} + \beta\phi\delta_{ij} \tag{10}$$

$$h_i = \alpha\phi_{,i} \tag{11}$$

$$g = -\omega\dot{\phi} - \xi\phi - \beta\varepsilon_{kk} \tag{12}$$

Here λ and μ are the Lamé constants; β is a coupling factor, which is a measure of the coupling between the displacement deformation and the change of the local volume fraction; α, ω and ξ are the "diffusion factor", they damping coefficient and the reflux factor of the change in the local volume fraction, respectively. Because the strain energy with respect to the reference configuration is positive definite, the coefficient λ, μ, α, β, ξ and ω depend on v_r and satisfy the following inequalities:

$$\begin{gathered} \mu \geqslant 0 \qquad \alpha \geqslant 0 \qquad \xi \geqslant 0 \qquad \omega \geqslant 0 \\ 3\lambda + 2\mu \geqslant 0 \qquad (3\lambda + 2\mu)\xi \geqslant 3\beta^2 \end{gathered} \tag{13}$$

In the absence of a body force b_i and ρl, the field equations governing the displacement field $u_i(\boldsymbol{x}, t)$ and the local volume fraction field $\phi(\boldsymbol{x}, t)$ are obtained by substituting the constitutive relations in Equations

10–12 into the equations of motion given by Equations 8 and 9 as

$$(\lambda + \mu)\nabla\nabla \cdot \boldsymbol{u} + \mu\nabla^2\mathbf{u} + \beta\nabla\phi = \rho\ddot{\boldsymbol{u}} \tag{14}$$

$$\alpha\nabla^2\phi - \omega\phi - \xi\phi - \beta\nabla \cdot \boldsymbol{u} = \rho\kappa\ddot{\phi} \tag{15}$$

These two equations, one vector and one scalar, represent a system of four scalar equations in four unknowns: ϕ and the three components of u_i. The boundary conditions on u_i are those of classical elasticity. The boundary condition on ϕ is

$$\boldsymbol{n} \cdot \nabla\phi = 0 \tag{16}$$

where **n** is the unit normal to the external boundary.

Plane acoustic waves are solutions of Equation 14 and 15 for which the displacement vector, u_i, and the volume fraction difference, ϕ, are of the form

$$u_i = Ad_iU(\boldsymbol{x}, t) \quad \phi = BU(\boldsymbol{x}, t) \tag{17}$$

where

$$U(\boldsymbol{x}, t) = \mathrm{Re}(\exp[\mathrm{i}(ft - \psi x_i)]) \tag{18}$$

Here d_i are the direction cosines of the displacement vector, $\boldsymbol{u}(\boldsymbol{x}, t)$, f is the frequency and ψ is a complex number such that Im $\psi < 0$. A and B are the amplitudes of the displacement and volume fraction change waves, respectively. Substitution of Equations 17 and 18 into Equations 14 and 15 yields

$$[(\lambda + 2\mu)\psi^2 - \rho f^2]A + \mathrm{i}\beta\psi B = 0 \tag{19}$$

$$(\alpha\psi^2 + \mathrm{i}\omega f - \rho\kappa f^2 + \xi)B - \mathrm{i}\beta\psi A = 0 \tag{20}$$

For the pair of Equations 19 and 20 to have a nontrivial solution for A and B we must set the determinant of their coefficients equal to zero; thus

$$[(\lambda + 2\mu)\psi^2 - \rho f^2](\alpha\psi^2 + \mathrm{i}\omega f + \xi - \rho\kappa f^2) - \beta^2\psi^2 = 0 \tag{21}$$

Equation 21 is the dispersion relation for the waves of the volume fraction. There are four wave velocities of interest. They are denoted by c_1 to c_4 and are defined as follows:

$$c_1 = \left(\frac{\mu}{\rho}\right)^{1/2} \quad c_2 = \left(\frac{\lambda + 2\mu}{\rho}\right)^{1/2} \quad c_3 = \left(\frac{\alpha}{\rho\kappa}\right)^{1/2}$$

$$c_4 = \frac{2\alpha}{l\omega} \tag{22}$$

These material parameters, which are defined as follows, are simple algebraic combinations of the material properties:

$$l_1 = \left(\frac{\alpha}{\beta}\right)^{1/2} \quad l_2 = \left(\frac{\alpha}{\xi}\right)^{1/2} \quad l_0 = \frac{\alpha}{\xi - \beta H}$$

$$H = \frac{\beta}{\lambda + 2\mu} \quad N = \frac{l_2^2}{l_1^2}H \tag{23}$$

Using the notations in Equations 22 and 23, Equation 21 can be rewritten as

$$\psi^4 - \left(\frac{f^2}{c_2^2} + \frac{f^2}{c_3^2} - \frac{1}{l_0^2} - \frac{\mathrm{i}\omega f}{\alpha}\right)\psi^2 + \frac{f^2}{c_3^2}\left(\frac{f^2}{c_3^2} - \frac{1}{l_2^2} - \frac{\mathrm{i}\omega f}{\alpha}\right) = 0 \tag{24}$$

Our analysis of the dispersion relation in Equation 24 will follow that of Puri [14] for thermoelastic waves. The information obtained from the dispersion relation includes the wavenumber, the wave speeds and the attenuation coefficient. The wavenumbers are the real part of ψ and the wave speeds are the frequency divided by the wavenumber. The attenuation coefficients are minus the imaginary part of ψ. Because the IF of foamed Al results from the change in the local distribution of the matrix, i.e., the dilatation and distortion of pores, the IF, Q^{-1}, can be written as

$$Q^{-1} = 2n4\pi a^2\ \Delta a\ \frac{\mathrm{Im}\ \psi}{\mathrm{Re}\ \psi} \tag{25}$$

Here n is the pore number per unit volume, a is the mean radius of pores and Δa is an increment of a. n is given by

$$n = \frac{3C}{4\pi a^3} \tag{26}$$

where C is the volume fraction of pores.

The two solutions of Equation 24 will be designated as ψ_e^2 and ψ_v^2. ψ_e^2 is associated with a wave that is predominantly an elastic wave and ψ_v^2 is associated with a wave that is predominantly a volume fraction wave. For high frequencies, from Equation 24, we can write

$$\psi_e = \frac{f}{c_2} - \mathrm{i}\,\frac{c_2^3c_3^4N\omega}{2(c_3^2 - c_2^2)l_2^2\alpha}\frac{1}{f^2} + \mathrm{O}\left(\frac{1}{f^3}\right) \tag{27}$$

$$\psi_v = \frac{f}{c_3} - \mathrm{i}\,\frac{1}{2}\frac{\omega}{\alpha}c_3 + \mathrm{O}\left(\frac{1}{f}\right) \tag{28}$$

Using Equations 26–28, Equation (25) can be written as

$$\begin{aligned} Q^{-1} &= Q_e^{-1} + Q_v^{-1} \\ &\approx \frac{3C}{4a}4\ \Delta a\ \frac{\omega c_3^2}{\alpha}\frac{1}{f} \\ &= \frac{3\omega}{\rho_m\kappa}\frac{C}{a(1 - C)}\frac{1}{f} \end{aligned} \tag{29}$$

Hence, $Q^{-1} \propto f^{-1}$, which is the main result of this section. From Equation 29, it can be seen that the IF is decreased as the frequency is raised. This is consistent with the experimental results as shown in Fig. 1. We therefore may draw the conclusions as follows. The IF is related to the pore size and the pore volume fraction or the porosity. For constant porosity and other identical condition a large pore size causes a smaller IF. This conclusion is consistent with the pore size dependence observed by Yu and He [3]. For constant pore size and other identical conditions a higher porosity causes a larger IF. This is consistent with the porosity dependence observed in this work and observed in the literatures [2, 4]. Using the data from Tables I and II, the IF was plotted versus pore parameters $C/a(1 - C)$ in Fig. 2. Fig. 2 shows that the IF is not a smooth linear function of the pore parameter $C/a(1 - C)$, but that fluctuations in the IF are observed. We believe that the fluctuations in the IF are caused by an inhomogeneous material distribution.

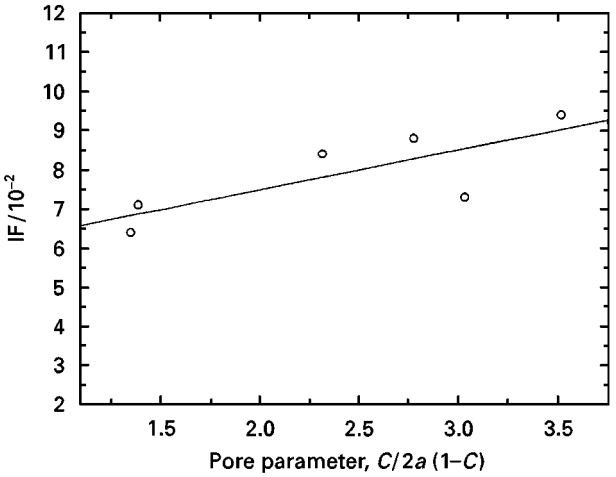

Figure 2 The relation between IF and pore parameter.

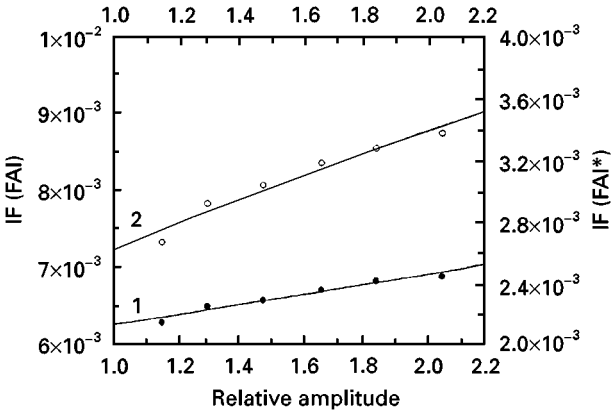

Figure 3 Strain-amplitude dependence of the IF of FAI* (●) and FA1 (○). Line 1, $y = 0.001\,78 + 0.000\,34x$; line 2, $y = 0.005\,75 + 0.001\,52x$.

Foamed Al is a statistical system and therefore a certain spatial variation in density and pore size cannot be avoided. The inhomogeneous distribution in the sample will give rise to changes in the porosity and pore size for any of samples and, correspondingly, lead to a change in the values of IF. We think that these changes will decrease if the samples are made larger, but in our case this is not possible owing to the limitations of experimental conditions (Recently, we measured the IF of large foamed Al specimens in a dynamic viscoelastic analyser (IMASS Company); the IF was a better linear function of the pore parameter $C/a(1 - C)$).

3.4. The amplitude effect of the internal friction of foamed Al

IF amplitude effects of FAl and FAl* are shown in Fig. 3 which shows that the IF is raised when the amplitude is raised. The IF of foamed Al depends non-linearly on the strain amplitude.

In order to study the non-linear dependence on amplitude, the resonant peak of foamed Al and the dependence of resonant frequency on amplitude were investigated. The relations between the square of the relative amplitude and the difference of excitation frequency with respect to the resonant frequency for sample FAl* and bulk Al are shown in Fig. 4. From this figure we can see that the resonant peak of foamed Al is asymmetric, whereas the resonant peak of bulk Al is symmetric.

For foamed and bulk Al the relations between the square of amplitude and the resonant frequency are shown in Fig. 5. For foamed Al, the resonance frequency decreases with increasing amplitude. For bulk Al, the resonant frequency is independent of the amplitude.

One distinguishing feature between linear and non-linear behaviour is the dependence of the frequency of the motion in non-linear vibration on the amplitude. For foamed Al, the equation of oscillations is non-linear whereas for bulk Al it is linear. On the basis of the considerations in Section 3.3, let us consider oscillations of foamed material. In solving the damping

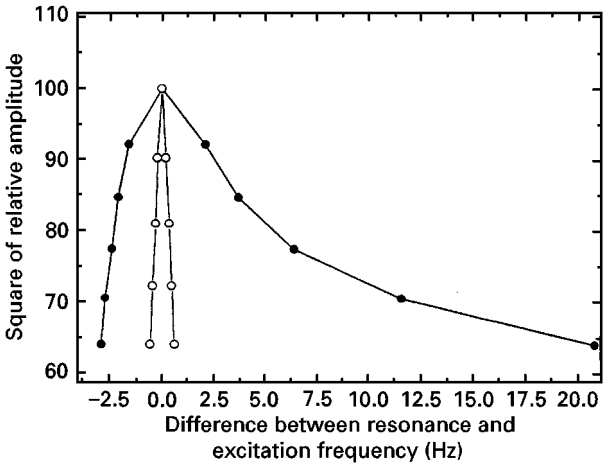

Figure 4 The relations between the square of relative amplitude and the difference between the excitation frequency and the resonant frequency (—●—), FA1* resonance frequency, 1010.4 Hz; (—○—) Al resonance frequency, 998.2 Hz.

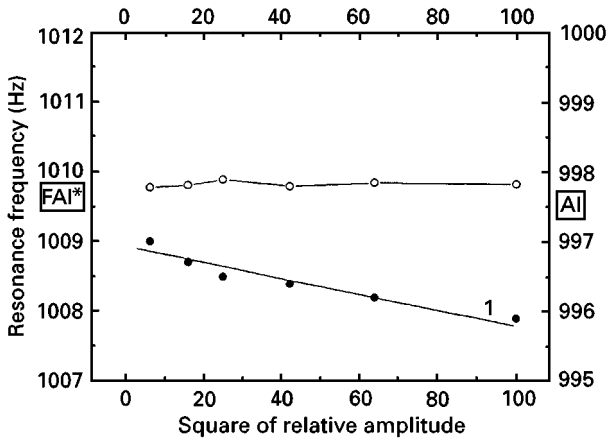

Figure 5 The relations between the square of the amplitude and the resonant frequency (—○—), AL; (●), FA1*; line 1, $Y = 1008.93–0.0114X$.

problem of forced oscillations, it is reasonable that the equation of the motion can be written as

$$\ddot{\phi} + 2\omega\dot{\phi} + f_0^2\phi = \frac{F}{m}\exp(\mathrm{i}ft) \qquad (30)$$

where ω is the damping coefficient, f_0 and f are the eigenfrequency and the excitation frequency, respectively, and F and m are the amplitude of the force and the mass, respectively. The equation of motion is linear. We seek a solution of the form $\phi = B\exp(i\delta)\exp(ift)$. We have

$$B = \frac{F}{m[(f_0^2 - f^2)^2 + 4\omega^2 f^2]^{1/2}} \tag{31}$$

For a given amplitude F of the force, the amplitude of the oscillation is greatest when

$$f = (f_0^2 - 2\omega^2)^{1/2} \tag{32}$$

Let us consider the range near resonance, putting $f = f_0 + \zeta$ with ζ small, and suppose that $\omega \ll f_0$. Then we can approximately put $f^2 - f_0^2 \approx 2f_0\zeta$ in Equation 31, so that

$$B^2 = \frac{F^2}{4m^2 f_0^2(\zeta^2 + \omega^2)} \tag{33}$$

It shows that the resonance curve is a symmetric curve with a maximum at the point $\zeta = 0$ (as shown in Fig. 6a). When the damping coefficient decreases, the resonance curve becomes more peaked. Using Equation 33, the IF can be written as

$$Q^{-1} = \frac{2\omega}{(f_0^2 - 2\omega^2)^{1/2}} \approx \frac{2\omega}{f_0} \tag{34}$$

When the anharmonic terms in the forced oscillations of a system are taken into account, the phenomena of resonance acquire new properties. The non-linearity of the damping oscillations results in the appearance of an amplitude dependence of the eigenfrequency or the resonant frequency, which is usually accompanied by an amplitude dependence of IF. As usual, there are three cases that result in non-linear oscillation. The resoring force is non-linear (hardening and softening), the damping force is proportional to the square of velocity and the damping force is related not only to the velocity but also to the displacement. Since the IF of foamed Al depends on the amplitude in the range of low frequency [3], we may think that the non-linearity of the oscillation does not result from the second case. If the non-linearity of the oscillation is caused by the first case, we write the amplitude dependence of the eigenfrequency as $f_0 + C_{an}B^2$, the constant C_{an} being the anharmonic coefficient [15]. Accordingly, we replace f_0 by $f_0 + C_{an}B^2$ in Equation 32. The resulting equation is

$$B^2 = \frac{F^2}{4m^2[(\zeta - C_{an}B^2)^2 + \omega^2]} \tag{35}$$

When the constant C_{an} is negative, the eigenfrequency decreases with increasing amplitude and the resonance curve is asymmetric (as shown in Fig. 6b), which is consistent with the experimental results shown in Fig. 4. According to Equation 34, the IF can be written as $Q^{-1} = 2\omega/(f_0 + C_{an}B^2)$. From Fig. 5, we can conclude that $C_{an}B^2$ is of the order of 1 Hz ($\ll f_0$). Hence, in this case the amplitude dependence of the IF can be ignored, which is in conflict with the experimental results shown in Fig. 3. From the consideration above, it might be the third case that results in the non-linearity of the oscillations. In Equation 30, the damping term, $2\omega\dot{\phi}$, will be rewritten as $2\omega\dot{\phi} = 2\omega_0\dot{\phi} + 2\omega_1\phi\dot{\phi}$. The non-linearity of the damping term results in the appearance of an amplitude dependence of the damping coefficient and it does not result in an amplitude dependence of the eigenfrequency but results in an amplitude dependence of the resonant frequency, f_r, which we write as

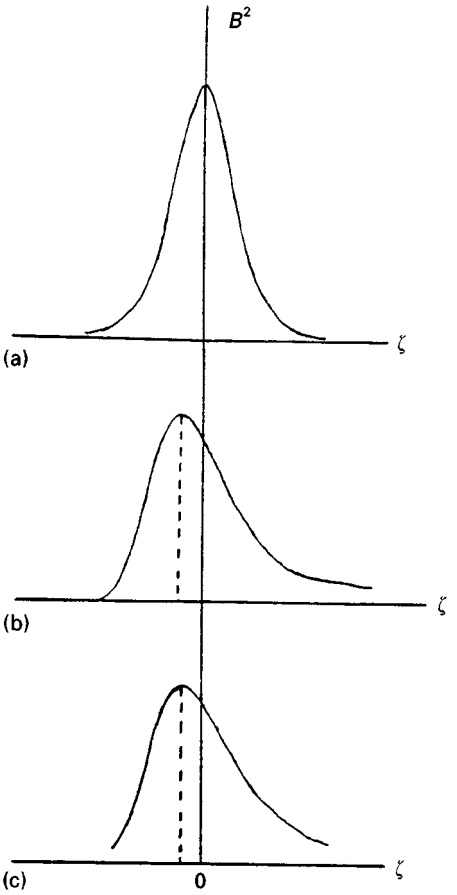

Figure 6 Schematic diagrams of resonance curves: (a) for a linear damping system with a linear softening restoring force; (b) for a linear damping system with a non-linear softening restoring force respectively; (c) for a non-linear damping system with a linear restoring force.

$$f_r = (f_0^2 - 2\omega^2)^{1/2} - C'_{an}B^2$$
$$\approx f_0 - \frac{2^{1/2}}{2}(\omega + C''_{an}\,2^{1/2}B^2) \tag{36}$$

According to Equation 32, we may write the amplitude dependence of the damping coefficient as

$$\omega = (\omega_0 + C'_{an}2^{1/2}B^2) = \omega_0(1 + C''_{an}B) \tag{37}$$

Thus the expressions for the amplitude and IF may be written as

$$B = \frac{F}{m[(f_0^2 - f^2)^2 + 4(\omega_0^2 + C'_{an}\,2^{1/2}B^2)f^2]^{1/2}} \tag{38}$$

$$Q^{-1} = \frac{2\omega_0(1 + C'_{an}B)}{f_r} \approx \frac{2\omega_0(1 + C''_{an}B)}{f_0} \tag{39}$$

According to Equations 36, 38 and 39, the resonant frequency is proportional to amplitude with a negative

slope, the resonant curve of oscillations of asymmetric as shown in Fig. 6c, and the IF is proportional to amplitude. This is in agreement with the experimental results shown in Figs 3–5. Therefore, on the basis of the above consideration and consideration in Section 3.3, the damping coefficients may be written as $[C/a(1-C)]\,\omega_0(1+C''_{an}B)$.

4. Conclusions

The IF of foamed Al was measured and its mechanisms were discussed. The non-linearity of oscillations of foamed Al was observed and analysed. The main results of the investigation are as follows.

1. The attenuation in foamed Al is not caused by the usual mechanism but by the pores. Pores in foamed Al may be high-energy dissipation resources. It is the change $\phi(x, t)$, in local volume fraction from the reference volume fraction that causes high-energy dissipation in foamed Al.

2. The IF of foamed Al increases with increasing porosity when the pore size is kept constant whereas, when the porosity is kept constant, it decreases with increasing pore size.

3. The IF of foamed Al decreases with increasing frequency in the range of high frequencies.

4. The IF is raised when the amplitude is raised.

5. The non-linearity of oscillations results from the non-linearity damping term.

6. The non-linear damping coefficient may be approximately expressed as $[C/a(1-C)]\omega_0(1+C''_{an}B)$, where a is the mean radius of pores, C is the volume fraction of pores, ω_0 is called the damping coefficient, C''_{an} is a constant and B is the amplitude of the oscillation.

References

1. G. J. DAVIES and Z. SHU, *J. Mater. Sci.* **18** (1983) 1989.
2. J. BANHART, J. BAUMEISTER, M. WEBER, *Mater. Sci. Engng* **A205** (1996) 221.
3. Q. X. YU and P. D. HE, *Mater. Mech. Engng* (*China*) **18** (1994) 26 (in Chinese).
4. J. BAUMEISTER, J. BANHART and M. WEBER, in Proceedings of the International Conference on Materials by Powder Technology, edited by F. Aldinger (DGM Informationsgesellschaft, Oberurzel, 1993) p. 501.
5. S. B. KULKARNI and P. RAMAKRISHANAN, *Int. J. Powder Met.* **9** (1973) 41.
6. J. P. DROLET, *Int. Powder Metall. Powder Technol.* **13** (1977) 222.
7. A. S. NOWICK and B. S. BERRY, "An elastic relaxation in crystalline solids", (Academic Press, New York, 1972) p. 628.
8. J. ZHANG, M. N. GUNDOR and E. J. LAVERNIA, *J. Mater. Sci.* **28** (1993) 1515.
9. T. MURA, "Micromechanics of defects in solids (Martinus Nijhoff, Dordrecht, 1987).
10. M. A. GOODMAN and S. C. COWN, *Arch. Rational. Mech. Anal.* **44** (1972) 249.
11. S. C. COWIN and J. W. NUNZIATO, *J. Elasticity* **13** (1983) 25.
12. P. PURI and S. C. COWIN, *ibid.* **15** (1985) 167.
13. J. W. NUNZIATO and S. C. COWIN, *Arch. Rational. Mech. Anal.* **72** (1979) 175.
14. P. PURI, *Int. J. Engng Sci.* **10** (1972) 467.
15. L. D. LANDAU and E. M. LIFSHITZ, "Mechanics", translated from the Russian by J. B. Sykes and J. S. Bell (Pergamon, Oxford, 3rd Edn., 1987) p. 88.

Received 29 April
and accepted 12 November 1997